



Pathogen transmission at stage-structured infectious patches: Killers and vaccinators



Thomas Caraco*, Wendy C. Turner

Department of Biological Sciences, University at Albany, Albany NY 12222, USA

ARTICLE INFO

Article history:

Received 6 March 2017

Revised 26 August 2017

Accepted 27 September 2017

Available online 28 September 2017

Keywords:

Free-living pathogen

Natural vaccination

Obligate killer

Virulence

ABSTRACT

Spatial localization of an obligate-killing, free-living pathogen generates a landscape of patches where new infections occur. As an infectious patch ages, both pathogen exposure at the patch and the probability of lethal infection following exposure can decline. We model stage-structured infectious patches, where non-lethal exposure can naturally “vaccinate” susceptible hosts. We let the between-stage difference in pathogen transmission, and then the between-stage difference in patch virulence, increase independently of other parameters. Effects of increasing either between-stage difference (about a fixed mean) depend on the probability a patch transitions from the first to second stage, *i.e.*, the chance that a killer patch becomes a vaccinator. For slower stage transition, greater between-stage differences decreased susceptibles, and increased both resistant-host and killer patch numbers. But our examples reveal that each effect can be reversed when between-stage transition occurs more rapidly. For sufficiently rapid stage transition, increased between-stage virulence differences can lead to pathogen extinction, and leave the host at disease-free equilibrium. The model's general significance lies in demonstrating how epidemiological variation among sites of environmentally transmitted disease can strongly govern host-parasite dynamics.

© 2017 Elsevier Ltd. All rights reserved.

1. Introduction

A number of important pathogens are transmitted through the physical environment; some have significance for wildlife conservation (Breban et al., 2010; Turner et al., 2013), and others infect human or agricultural hosts (Moore et al., 2014; Turner et al., 2006). Environmental transmission, by definition, requires that the pathogen persist outside of host tissues, and many such pathogens have a free-living, infectious form capable of lengthy survival in the abiotic environment (Dwyer, 1992; Godfray et al., 1997). A persistent free-living stage can maintain the pathogen population through periods of low host density (Caraco and Wang, 2008; Walther and Ewald, 2004), and may relax epidemiological constraints on the evolution of virulence (Cressler et al., 2015; Day, 2002; Gandon, 1998).

Models for the evolutionary ecology of environmentally transmitted disease usually assume that a free-living pathogen, when released from an infected host, enters a homogeneously mixed pool. Within the pool, all pathogen particles (of a given strain) have the same longevity, the same rate of contacting hosts, and the

same infectiousness upon contact (Alizon and Michalakakis, 2015). That is, theory for disease transmission through the abiotic environment generally assumes that pathogens lack ecological or demographic structure. But, for many free-living pathogens, host contacts occur heterogeneously in space or time (Caraco et al., 2016; Duryea et al., 1999; Roche et al., 2011). A consequence of this heterogeneity, upon which our study rests, is that infectious contacts with a free-living pathogen may often be structured with respect to both transmission and virulence.

Spatial clustering of environmental transmission commonly occurs when a pathogen must kill its current host to infect another; most obligate killers release infectious propagules only at the demise of diseased hosts (Ebert and Herre, 1996). For example, polyhedrosis virus kills moth larvae, and then viral particles are deposited on the leaf where the larva died. Subsequent infection occurs when another larva feeds on the same leaf (Dwyer, 1994; Reeson et al., 2000). *Bacillus anthracis* has been studied in wildlife, particularly the plains zebra (*Equus quagga*). Infected herbivores may die a few days after exposure to the pathogen (Bagamian et al., 2013). Carcasses exsanguinate, producing localized patches of *B. anthracis* spores. Nutrients from a carcass generate a local pulse of plant growth, which attracts herbivores to the infectious patch (Turner et al., 2014). Patches can persist for a decade, but spore density within a given patch declines with

* Corresponding author.

E-mail addresses: caraco@albany.edu (T. Caraco), wcturner@albany.edu (W.C. Turner).

time (Turnbull, 2008), and the local vegetation returns to its initial state within a few years. Each example highlights association of an obligate-killing pathogen with localized propagule concentrations where environmental transmission occurs. As propagules decay within patches, their level of infectiousness and severity of impact on infected hosts should decline (Turner et al., 2016). Below we argue that ecological heterogeneity among sites of environmentally transmitted infection have significant implications for pathogen invasion and endemic disease levels.

Our study focuses on two general questions. After developing a model for stage-structured infectious patches, we first ask how increasing the between-stage difference in infectiousness, and (then) the between-stage difference in virulence, impacts host population size and the number of pathogen patches. Secondly, we explore the “killer-vaccinator” hypothesis (Cizauskas et al., 2014). Populations of some environmentally transmitted pathogens may include newer patches that kill the majority of hosts they infect. Older patches, where infectious propagule densities are reduced (Turner et al., 2016), may commonly induce acquired resistance and so vaccinate more often than kill. Stated simply, resistance among hosts might be promoted by an increased frequency of latter-stage, lower-virulence patches.

1.1. Organization

Section 2 develops a model in which seasonality separates host intraspecific competition from infection and disease. Coupling seasonal processes yields a dynamics for susceptible and resistant hosts, and for a stage-structured population of infectious patches. Section 3 analyzes disease-free growth of the host population, and outlines how killer-vaccinator differences can affect the pathogen’s advance when rare. Section 4 lists the fixed-point endemic equilibria, which we use to study consequences of the pathogen’s stage structure. Sections 5 through 7 present the main results; we consider (1) between-stage differences in transmission rates, by (2) between-stage differences in the probability of fatal infection, and (3) functional dependence of virulence and persistence of killer-stage patches. The term “greater structure” implies increased between-stage differences in these traits; as virulence structure increases, newer patches more frequently kill, and older patches more frequently vaccinate.

Our overall objective is understanding how between-stage differences in transmission and virulence discriminate the disease-free state from an endemically infected host population. Our general result finds that when killer patches tend to remain virulent across host generations, increasing between-stage differences decreases numbers of susceptibles, and increases numbers of resistant hosts and both patch stages. However, when killers transition sufficiently rapidly to the less virulent stage, each effect of structure is reversed, and sufficiently strong stage structure can result in pathogen extinction.

2. Model

Most vertebrates breed seasonally, so we model an annual cycle of wet and dry seasons (Havarua et al., 2014; Sinclair et al., 2000). During the wet season, vertebrate hosts experience infectious contacts with the free-living pathogen, some of which lead to fatal disease. Carcasses resulting from mortal infections become new pathogen patches the following year (Turner et al., 2016). During the dry season, the herbivorous hosts compete for limited resources, implying density-dependent reproduction. Infectious patches may decay (i.e., disappear) as a consequence of abiotic conditions during the dry season. A fraction of surviving, highly virulent patches transitions to a less virulent stage.

Table 1

Definitions of model variables and symbols. Top: host population; middle: structured patches; bottom: vector-valued parameters.

Symbols	Definitions
S_t	Number of susceptible hosts, dry season, time t
R_t	Number of resistant hosts, dry season, time t
σ_t	Number of susceptible hosts entering wet season, time t
ρ_t	Number of resistant hosts entering wet season, time t
g	Proportional survival among hosts, dry season
γ	Proportional loss of resistance among R_t hosts
λ	Host natality
μ	Scales density-dependence of host natality
i	Index of wet-season host category; $i = \sigma, \rho$
x	Index of patch stage; $x = 1, 2$
$P_{x,t}$	Number of stage- x infectious patches, dry season, time t
$\pi_{x,t}$	Number of stage- x infectious patches entering wet season, time t
ξ_x	Probability that a stage- x patch persists through dry season
q_{12}	Frequency of stage-1 to stage-2 transition among persisting $P_{1,t}$
β_x	Transmission, each stage- x patch; integrates encounter rate and chance of infection
$v_{\sigma,x}$	Disease-mortality probability for susceptibles infected at a stage- x patch
$v_{\rho,x}$	Disease-mortality probability for resistant hosts infected at a stage- x patch
θ_t	$\beta_1\pi_{1,t}/(\beta_1\pi_{1,t} + \beta_2\pi_{2,t})$
\mathbf{H}_t	$\{\theta_t, 1 - \theta_t\}$
\mathbf{V}_σ	$\{v_{\sigma,1}, v_{\sigma,2}\}$
\mathbf{Z}_σ	$\{1 - v_{\sigma,1}, 1 - v_{\sigma,2}\}$
\mathbf{V}_ρ	$\{v_{\rho,1}, v_{\rho,2}\}$
\mathbf{Z}_ρ	$\{1 - v_{\rho,1}, 1 - v_{\rho,2}\}$

Year t begins at the start of a dry season. S_t represents the number of susceptible hosts, and R_t is the number of (partially) resistant hosts, entering the dry season. Resistance implies that the individual was exposed to the pathogen during the previous wet season, but recovered (or seroconverted) and retains some adaptive immunity. $P_{x,t}$ is the number of infectious patches at the start of the dry season; $x = 1, 2$. Table 1 defines symbols.

2.1. Host reproduction, patch decay

During the dry season the number of susceptible hosts changes through non-disease mortality and loss of immunity among resistant hosts. A birth pulse at the beginning of the wet season (Gasaway et al., 1996) increases the number of susceptibles; all newborns enter the susceptible class. Collecting these changes, a total of σ_t susceptible hosts may be exposed to infection during the wet season:

$$\sigma_t = g(S_t + \gamma R_t) + \lambda(S_t + R_t)e^{-\mu(S_t + R_t)} \quad (1)$$

g is the fraction of all hosts ($S_t + R_t$) that survive the dry season; $0 < g < 1$. γ is the proportion of the surviving R_t hosts that lose resistance and return to the susceptible class. λ is the finite rate of increase, and host self-regulation has a Ricker form (Avilés, 1999; Trainor and Caraco, 2006). Density-dependence is a function of the number of hosts alive at the start of the dry season; the strength of self-regulation increases with μ .

The number of resistant hosts changes during the dry season through mortality and loss of resistance. Thereafter, ρ_t resistant hosts enter the wet season: $\rho_t = g(1 - \gamma)R_t$.

The $P_{x,t}$ also change during the dry season; some patches decay, and some stage-1 patches enter stage-2. $\pi_{x,t}$ patches of stage- x enter the wet season. For the first stage, $\pi_{1,t} = \xi_1(1 - q_{12})P_{1,t}$, and for the second stage, $\pi_{2,t} = \xi_1q_{12}P_{1,t} + \xi_2P_{2,t}$. ξ_x is the fraction of stage- x patches persisting through the dry season, and q_{12} is the fraction of surviving stage-1 patches that transition to stage-2. The ξ_x depend on exogenous abiotic factors. Transition of a patch

to stage-2 represents reduction in the concentration of infectious propagules within the patch.

2.2. Infection dynamics

The plains zebra-*Bacillus anthracis* interaction (Gasaway et al., 1996; Turner et al., 2014) suggests some details, but the addition of population structure to models of environmentally transmitted infections has general implications. If a susceptible host acquires an infection during the wet season, it either recovers with resistance or dies. Resistant hosts that avoid infection lose their partial immunity (Cizauskas et al., 2014). Completing the annual cycle, S_{t+1} is the number of hosts that avoid infection during the wet season:

$$S_{t+1} = e^{-(\beta_1\pi_{1,t} + \beta_2\pi_{2,t})} (\sigma_t + \rho_t) = e^{-(\beta_1\pi_{1,t} + \beta_2\pi_{2,t})} ([S_t + R_t][g + \lambda e^{-\mu(S_t + R_t)}]) \quad (2)$$

We treat encounters with stage- x infectious patches as independent Poisson processes. $\beta_x \pi_{x,t}$ is the rate at which any host, susceptible or resistant, experiences infectious contact at a stage- x pathogen patch ($x = 1, 2$). During any wet season, an individual host acquires at most a single infection, and then either dies or develops transient immunity. That is, ‘exposure’ without a chance of lethal infection is irrelevant to the dynamics.

Each β_x is a stage-specific transmission rate. Our model treats transmission as a combination of attraction to patches (where hosts encounter the pathogen) and the chance of infection within patches. Each component of transmission should scale positively with spore density, and the relative recency of stage-1 patches implies that infectious-spore densities will be greater in the first stage (Turner et al., 2016). Therefore, we take $\beta_1 \geq \beta_2$. That is, we assume that the attractiveness of forage quality increases the rate at which hosts encounter stage-1 patches, and, secondly, that the likelihood of infection, given encounter, will be greater in stage-1 patches.

When infection occurs, we take its virulence as the probability that the infected host dies. Virulence depends on both the host and patch stage, and we use these probabilities to complete the annual cycle for resistant hosts:

$$R_{t+1} = [1 - e^{-(\beta_1\pi_{1,t} + \beta_2\pi_{2,t})}] \{ \sigma_t [(1 - \nu_{\sigma,1})\theta_t + [1 - \nu_{\sigma,2}][1 - \theta_t]] + \rho_t [(1 - \nu_{\rho,1})\theta_t + [1 - \nu_{\rho,2}][1 - \theta_t]] \}$$

$\nu_{\sigma,x}$ is virulence when susceptible hosts incur stage- x infections; $\nu_{\rho,x}$ is virulence among resistant hosts infected at a stage- x patch. By the definition of resistance, $\nu_{\rho,x} < \nu_{\sigma,x}$. That is, resistant hosts are less likely than susceptibles to succumb to infection. Any infection not leading to mortality leaves the host with temporary resistance (Bagamian et al., 2013).

Outcomes of infectious exposure must be weighted by the encounter rates with the different patch stages: $\theta_t = \beta_1\pi_{1,t} / (\beta_1\pi_{1,t} + \beta_2\pi_{2,t})$. Substituting for wet-season densities and simplifying yields the annual dynamics $R_{t+1}(S_t, R_t, \theta_t)$:

$$R_{t+1} = [1 - e^{-(\beta_1\pi_{1,t} + \beta_2\pi_{2,t})}] \times \{ [g(S_t + \gamma R_t) + \lambda(S_t + R_t)e^{-\mu(S_t + R_t)}] \times (\mathbf{Z}_\sigma \cdot \mathbf{H}_t) + g(1 - \gamma)R_t(\mathbf{Z}_\rho \cdot \mathbf{H}_t) \} \quad (3)$$

where $(\mathbf{Z}_i \cdot \mathbf{H}_t)$ is a scalar product.

The number of stage-1 patches sums stage-1 patches that persisted through the last dry season without transition, plus new patches generated at carcass sites during the wet season:

$$P_{1,t+1} = \pi_{1,t} + [1 - e^{-(\beta_1\pi_{1,t} + \beta_2\pi_{2,t})}] \{ \sigma_t [\nu_{\sigma,1}\theta_t + \nu_{\sigma,2}(1 - \theta_t)] + \rho_t [\nu_{\rho,1}\theta_t + \nu_{\rho,2}(1 - \theta_t)] \}$$

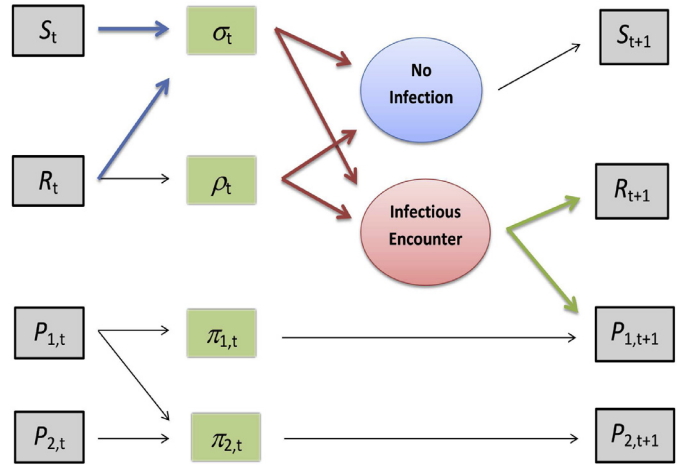


Fig. 1. Annual cycle. S_t (σ_t) is susceptible count for dry (wet) season. R_t (ρ_t) counts resistant hosts at dry (wet) season. $P_{x,t}$ ($\pi_{x,t}$) counts stage- x patches at dry (wet) season. Density-dependent interactions indicated by wider arrows; thin arrows indicate density-independent transitions.

Substituting for wet-season counts gives the annual dynamics $P_{1,t+1}(S_t, R_t, \theta_t)$:

$$P_{1,t+1} = \xi_1(1 - q_{12})P_{1,t} + [1 - e^{-(\beta_1\pi_{1,t} + \beta_2\pi_{2,t})}] \times \{ [g(S_t + \gamma R_t) + \lambda(S_t + R_t)e^{-\mu(S_t + R_t)}] \times (\mathbf{V}_\sigma \cdot \mathbf{H}_t) + g(1 - \gamma)R_t(\mathbf{V}_\rho \cdot \mathbf{H}_t) \} \quad (4)$$

Environmental transmission occurs only at infectious patches, and not through insect vectors or contact with carcasses (Friedman and Yakubu, 2013). Virulence of stage-1 patches is greater: $\nu_{i,1} > \nu_{i,2}$ for $i = \sigma, \rho$. Greater density of the pathogen within stage-1 patches increases the chance that an infection acquired there proves lethal. The number of stage-2 patches at time $(t + 1)$ sums transitions from persisting stage-1 patches plus stage-2 patches that survived the last dry season:

$$P_{2,t+1} = \pi_{2,t} = \xi_1 q_{12} P_{1,t} + \xi_2 P_{2,t} \quad (5)$$

Since stage-1 patches are more virulent, q_{12} is, metaphorically, the probability that a surviving killer becomes a natural vaccinator (Pujol et al., 2009). Fig. 1 shows a flowchart of the model's dynamics.

2.2.1. Model summary

Intraspecific competition and disease mortality regulate host population growth. Their relative strengths should govern population sizes and, more generally, the system's dynamic complexity; see Appendix A. The annual cycle assumes that host self-regulation acts before mortality from infection. Hence, the ‘Ricker term,’ $e^{-\mu(S_t + R_t)}$, appears in the dynamics of both host classes, and in the dynamics of $P_{1,t}$. Essentially, competition limits the number of hosts available to the pathogen, and so diminishes the destabilizing effects of disease (Cavaliere and Kocak, 1999; May et al., 1981).

Our model is novel in that it considers stage-structured pathogen-transmission, combined with natural vaccination. For many infectious diseases, acquisition of resistance occurs only after a host has contributed to further infections, via direct contact or shedding into the environment. Our model considers a distinctly different dynamics; natural vaccination (a susceptible to resistant transition) implies that a living host bypasses an infectious state. The stage-structured disease dynamics will generally exhibit greater complexity than the associated, unstructured model, as found in predator-prey models with age or stage-structured consumers (McCauley et al., 1993). For completeness,

Appendix B presents the reduced version of our model where all patches are identical.

3. Pathogen rarity

In the absence of disease, density-dependent natality regulates host numbers. If host extinction is unstable, the positive equilibrium node is $S_{DF}^* = [\ln(\lambda) - \ln(1 - g)]/\mu$; the subscript identifies the disease-free equilibrium. S_{DF}^* will be locally stable if $0 < \ln(\lambda) - \ln(1 - g) < 2/(1 - g)$. Greater dry-season survival can stabilize S_{DF}^* by relaxing overcompensation. Increased natality, of course, can be destabilizing. For sufficiently large (λ/μ) the model should belong to the class of one-dimensional maps exhibiting the period-doubling route to chaos (Kaplan and Glass, 1995); see Appendix C.

3.1. On pathogen invasion

Suppose that we introduce the pathogen into a disease-free host population as a single carcass, which becomes a stage-1 patch next wet season. The patch remains in the first stage for τ_1 wet seasons ($\tau_1 = 1, 2, \dots$). τ_1 has a geometric distribution with mean $\langle \tau_1 \rangle = [1 - \xi_1(1 - q_{12})]^{-1}$. The initial stage-1 patch ultimately decays or transitions to the second stage; the probability that the patch ever reaches stage-2 is then $\xi_1 q_{12}/(\xi_1 q_{12} + 1 - \xi_1)$. Given transition to stage-2, the patch persists for τ_2 wet seasons. τ_2 has expectation $\langle \tau_2 \rangle = (1 - \xi_2)^{-1}$. The wet season population in the absence of disease mortality is $\sigma^* = S_{DF}^*(g + \lambda e^{-\mu S_{DF}^*}) = S_{DF}^*$.

Our model permits acquisition of resistance, via natural vaccination, without contributing to the spread of disease. This complicates the dynamics of the rare, obligate-killing pathogen; traits that increase disease mortality (producing new infectious patches) may also increase the frequency of resistance among hosts. Natural vaccination may impede pathogen invasion. Here, we ignore resistance and present a simple upper bound on patch-growth when rare.

Neglecting resistance, the expected number of patches generated over the lifetime of the initial infectious patch is:

$$\mathfrak{N}^u = S_{DF}^* \left\{ \frac{(1 - e^{-\beta_1})v_{\sigma,1}}{[1 - \xi_1(1 - q_{12})]} + \frac{\xi_1 q_{12}}{\xi_1 q_{12} + 1 - \xi_1} \frac{(1 - e^{-\beta_2})v_{\sigma,2}}{(1 - \xi_2)} \right\} \tag{6}$$

$\mathfrak{N}^u < 1$ is a sufficient, but not necessary, condition for pathogen extinction, since \mathfrak{N}^u exceeds the expected number of patches per patch when hosts acquire resistance. Because the pathogen is an obligate-killer, greater virulence always increases \mathfrak{N}^u , in the absence of dependence between pathogen traits (Caraco et al., 2014; Day, 2002). As the between-stage transition probability q_{12} increases, the second stage contributes more, and the first stage contributes fewer, fatal infections to \mathfrak{N}^u . Since $v_{\sigma,2} < v_{\sigma,1}$, the net effect (depending on the ξ_x) can reduce \mathfrak{N}^u .

4. Fixed-point equilibria

This section restricts attention to fixed-point equilibria with the host extant. Suppose we hold all parameters but the transmission rates β_x constant. If β_1 and β_2 are sufficiently small, the host population remains disease-free, and the stable equilibrium node has $S_{DF}^* > 0$, with $R^* = P_1^* = P_2^* = 0$.

Increased transmission permits pathogen invasion, so that the P_x have positive equilibrium densities. When $[S^*R^*P_1^*P_2^*] > 0$, we have an interior equilibrium, which we evaluate numerically. If self-regulation is not too strong (μ not too large), then $\exp(-\mu(S^* + R^*)) \approx 1 - \mu(S^* + R^*)$. At positive equilibrium

the number of host births equals the number of deaths, so that we can approximate the ratio of killer patches to hosts:

$$\frac{P_1^*}{S^* + R^*} \approx \frac{\lambda(1 - \mu) + g - 1}{1 - \xi_1(1 - q_{12})} \tag{7}$$

Increased natality λ increases the killer-to-host ratio. If infectious patches better survive abiotic challenge (ξ_1 increases) the ratio again increases. An increase in the between-stage transition probability q_{12} changes stage structure, and reduces the number of stage-1 patches per host.

All infections are mortal at one boundary equilibrium. If $v_{\sigma,1} = v_{\sigma,2} = 1$, then no infected host survives disease and $R^* = 0$. When dry-season survival is sufficiently smaller than the annual number of offspring per host at equilibrium ($g < \lambda \exp\{-\mu S^*\}$), we can approximate this equilibrium node. Since $g < 1$ by definition, and host reproduction compensates for disease mortality, the approximation should be reasonable. At the “maximal virulence” equilibrium infections are not too common, but always lethal:

$$S^* \approx \frac{\ln[\lambda] - (\beta_1 \pi_1^* + \beta_2 \pi_2^*)}{\mu} \tag{8}$$

$$R^* = 0 \tag{9}$$

$$P_1^* \approx \frac{e^{(\beta_1 \pi_1^* + \beta_2 \pi_2^*)} - 1}{1 - \xi_1(1 - q_{12})} \frac{\ln[\lambda] - (\beta_1 \pi_1^* + \beta_2 \pi_2^*)}{\mu} \tag{10}$$

$$P_2^* = P_1^* \frac{\xi_1 q_{12}}{1 - \xi_2} \tag{11}$$

Since we focus on pathogen population structure, we assume that $1 > v_{\sigma,1} \geq v_{\sigma,2}$ for the rest of the paper, and ignore the case where all infections are mortal.

As transmission rates β_x continue to increase, $S^* \rightarrow 0$. In the limit, the host population, at the beginning of the dry season, includes only resistant individuals. Equivalently, neither newborns nor surviving resistant hosts escape contact with the pathogen during the wet season. At this limit we have the “maximal-exposure” boundary equilibrium:

$$S^* = 0 \tag{12}$$

$$R^* = \frac{\ln[\lambda(\mathbf{Z}_\sigma \cdot \mathbf{H}^*)] - \ln[1 - g(\gamma(\mathbf{Z}_\sigma \cdot \mathbf{H}^*) + (1 - \gamma)(\mathbf{Z}_\rho \cdot \mathbf{H}^*))]}{\mu} \tag{13}$$

$$P_1^* = R^* \frac{(g\gamma + \lambda e^{-\mu R^*})(\mathbf{V}_\sigma \cdot \mathbf{H}^*) + g(1 - \gamma)(\mathbf{V}_\rho \cdot \mathbf{H}^*)}{1 - \xi_1(1 - q_{12})} \tag{14}$$

$$P_2^* = P_1^* \frac{\xi_1 q_{12}}{1 - \xi_2} \tag{15}$$

π_1^* and π_2^* are the equilibrium patch numbers during the wet season, and at equilibrium $\theta_1^* = \beta_1 \pi_1^*/(\beta_1 \pi_1^* + \beta_2 \pi_2^*)$. The maximal-exposure equilibrium depends on θ_1^* , which simplifies to:

$$\theta_1^* = \beta_1(1 - q_{12}) / \left(\beta_1(1 - q_{12}) + \beta_2 \left[\frac{q_{12}}{1 - \xi_2} \right] \right) \tag{16}$$

Then vector \mathbf{H}^* then is $[\theta_1^*, 1 - \theta_1^*]$. Intuitively, θ_1^* increases with β_1 , and decreases with both β_2 and ξ_2 . Computationally, we report the maximal-exposure equilibrium when $S^* < 1$.

Fig. 2 shows regions of the model’s stable point equilibria. In each plot, as transmission rates β_x increase, the disease-free equilibrium gives way to the interior equilibrium, which in turn yields

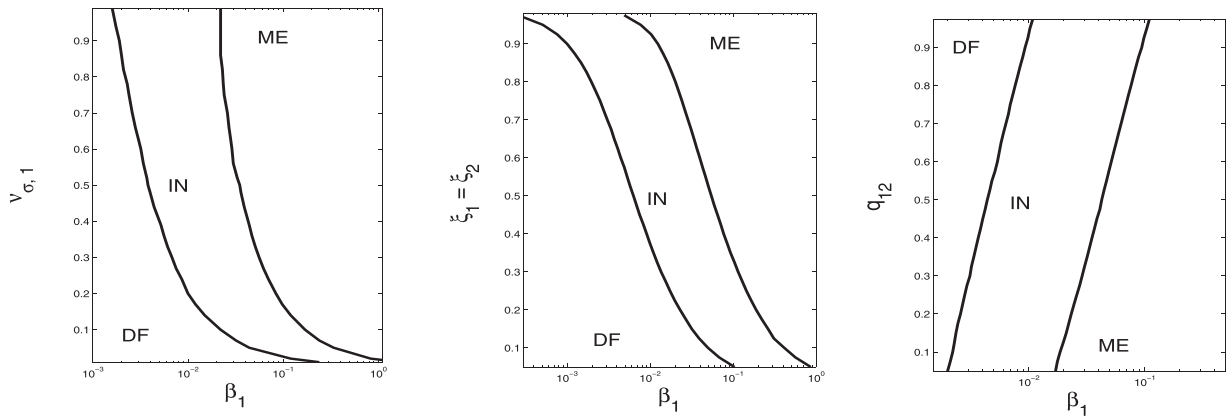


Fig. 2. Point equilibria: disease-free (DF), interior (IN), and maximal exposure (ME). All plots: $\lambda = 3$, $g = 0.6$, $\mu = 0.005$, $\gamma = 0.7$, and $\beta_2 = \beta_1/2$; $v_{\sigma,2} = v_{\sigma,1}/3$, $v_{\rho,1} = v_{\sigma,1}/2$, and $v_{\rho,2} = v_{\sigma,1}/6$. Left plot: $\xi_1 = \xi_2 = 0.7$, $q_{12} = 0.3$. Center plot: $q_{12} = 0.3$, $v_{\sigma,1} = 0.6$. Right plot: $\xi_1 = \xi_2 = 0.7$, $v_{\sigma,1} = 0.6$. Equilibria locally stable (numerical checks).

to the maximal-exposure equilibrium. Increasing either the virulence of infections (left plot) or the survival of pathogen patches (center plot) decreases both the minimal transmission required for pathogen invasion and the levels of transmission necessary for maximal exposure. However, increasing q_{12} , the stage-1 to stage-2 transition probability (right plot), has the opposite effects. A larger q_{12} can reduce the mean virulence across all pathogen patches, hindering the pathogen's invasion of a disease-free host population.

5. Structured transmission

Our study explores ecological consequences of varying between-stage differences in demographic/epidemiological parameters. To vary transmission structure, we let $\beta_1 = (\beta_0/2) + \delta_\beta$, and $\beta_2 = (\beta_0/2) - \delta_\beta$. Structure increases as $\beta_1 - \beta_2 = 2\delta_\beta \geq 0$ increases. That is, greater structure increases transmission per stage-1 patch (β_1), and decreases transmission per stage-2 patch (β_2) about a fixed mean. We emphasize interaction of structured transmission and the between-stage transition probability q_{12} . Fig. 3 shows an example of equilibrium host and patch counts as bivariate functions of δ_β and q_{12} . At any interior equilibrium, increasing q_{12} increases the number of susceptibles, and decreases numbers of both resistant hosts and stage-1 patches (killers). The count of stage-2 patches (vaccinators) first increases and then declines across levels of q_{12} . Since P_1^* must decline as increasing q_{12} alters patch-stage structure, effects on susceptible and resistant hosts follow logically. At low q_{12} , P_1^* is sufficiently large that the decline in stage-1 patches with greater q_{12} generates more stage-2 patches. But at high q_{12} , P_1^* declines sharply with the average virulence across host infections; disease mortality has a lesser role in regulating host population dynamics. Here, increases in q_{12} , via the consequent decline in P_1^* generate reductions in P_2^* .

More interestingly, effects of transmission structure δ_β depend on the value of q_{12} . When persisting stage-1 patches tend to remain in the more virulent state ($q_{12} < 1/2$) increased δ_β reduces the count of susceptibles, and increases the absolute number of resistant hosts; simultaneously, both patch stages (gently) increase in number. However, when persisting stage-1 patches more rapidly transition to the less virulent state ($q_{12} > 1/2$) each effect is reversed. Greater structure reduces patch numbers; consequently, susceptible host numbers increase while the number of resistant hosts declines with δ_β . For the parameters used in Fig. 3, combinations of rapid stage-transition and relatively large δ_β invert the stage structure, so that $P_2^* \geq P_1^*$ at internal equilibrium. Additional

increase in either transmission structure or q_{12} now can drive the system to the disease-free state.

The same patterned response to q_{12} emerges in the frequency of resistance among hosts, $R^*/(S^* + R^*)$, and disease mortality; see Fig. 4. At low q_{12} , greater transmission structure increases the fraction of the host population suffering mortal infection (DM), and most hosts entering the dry season are resistant. Both the absolute number and relative frequency of resistant hosts are maximal where the count of killer patches is maximal and the count of susceptibles is minimal, contrary to the “killer-vaccinator” hypothesis. However, at high q_{12} increasing δ_β produces a decline in both resistance frequency and disease mortality. Proportional mortality due to infection provides an index of the pathogen's impact on host population dynamics; regulation of the host by disease disappears when both δ_β and q_{12} become sufficiently large.

A general question raised by these examples asks how greater difference in stage-specific transmission may exert contrasting effects on populations at low versus high q_{12} . A more particular, related question asks why the pathogen may fall to extinction when both δ_β and q_{12} become sufficiently large. When patches are similar (low δ_β) the disease dynamics should respond more slowly to an increase in q_{12} , since the environment-wide transmission level declines slowly as q_{12} increases. Greater between-stage transmission differences (high δ_β) promote faster change in equilibrium populations as q_{12} increases. This does not, however, explain contrasting effects of δ_β across levels of q_{12} . Recall \mathfrak{R}^u , an upper bound on pathogen growth when rare. The response of \mathfrak{R}^u to change in β_1 , given that $\beta_1 + \beta_2 = \beta_0$ (a constant), yields an approximate answer to both questions. Along the constraint on the β_x , $\partial \mathfrak{R}^u / \partial \beta_1$ has the sign of:

$$\phi_\beta = \frac{v_{\sigma,1}}{v_{\sigma,2}} e^{-\beta_1} - \frac{\xi_1 q_{12}}{1 - \xi_2} e^{\beta_1 - \beta_0} \tag{17}$$

$\xi_1 q_{12}$ is the fraction of stage-1 patches that survive and transition to stage-2 during the dry season. At low q_{12} , ϕ_β should be positive, indicating that pathogen growth increases with β_1 (hence with δ_β). But at high q_{12} , ϕ_β can become negative, and greater δ_β can now reduce pathogen growth. Since $\beta_1 < \beta_0$ in our example, there should always be a sufficiently large between-stage virulence ratio ($v_{\sigma,1}/v_{\sigma,2}$) to insure $\phi_\beta > 0$.

6. Structured virulence

Virulence structure increases with the between-stage difference ($v_{i,1} - v_{i,2}$) for $i = \sigma, \rho$. We set $v_{\sigma,1} = v_0 + \delta_v$, and $v_{\sigma,2} = v_0 - \delta_v$. As a convenience, we let $v_{\rho,x} = kv_{\sigma,x}$, where $0 < k < 1$. As structure

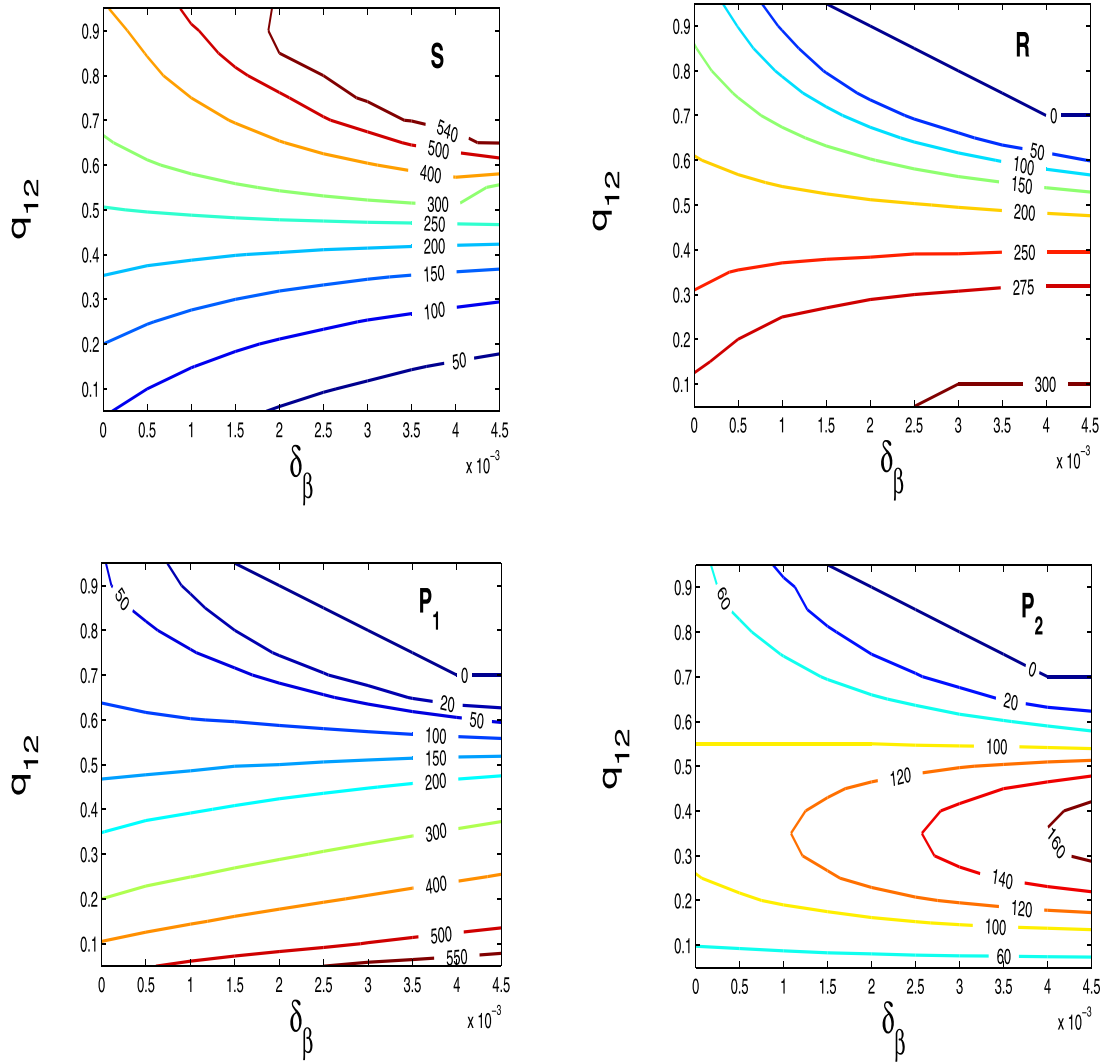


Fig. 3. Structured transmission. Contours: equilibrium susceptible count (upper left), resistant hosts (upper right), first-stage patches (lower left), and second-stage patches (lower right). $\beta_1 = 0.005 + \delta_\beta$; $\beta_2 = 0.005 - \delta_\beta$. Each plot: $\lambda = 3$, $\mu = 0.005$, $g = \gamma = 0.8$, $\xi_1 = \xi_2 = 0.6$, $\nu_{\sigma,1} = 0.6$, $\nu_{\sigma,2} = 0.3$, $\nu_{\rho,1} = 0.4$, $\nu_{\rho,2} = 0.1$. Each plot: disease-free equilibrium in upper right corner.

δ_ν increases, lethal-infection frequency grows in stage-1 patches, for both susceptible and resistant hosts, and the frequency of mortal infections declines in stage-2 patches.

Fig. 5 shows equilibrium population sizes as bivariate functions of δ_ν and q_{12} . Any increase in the between-stage transition probability q_{12} increases susceptibles and decreases both resistant-host and stage-1 patch counts. Changes in host numbers follow directly from reduction in the mean virulence experienced across all patches, and the consequent reduction in patch numbers. The count of stage-2 patches (again) attains a maximum at intermediate q_{12} .

Effects of virulence structure in our example depend on q_{12} , much as above. At low q_{12} susceptible hosts decrease, while resistant hosts and both patch types increase in number as between-stage virulence differences increase. Extending the duration of the first stage allows persistent killers to exert a stronger regulatory effect on the host population. At high q_{12} these effects are reversed. Increasing the between-stage virulence difference, given the reduced frequency of killer patches in the pathogen population, reduces disease mortality. Fast transition between stages, altering the pathogen's population structure, combined with larger δ_ν , drives the pathogen to extinction, leaving the host at the disease-free equilibrium.

Fig. 6 shows the frequency of resistance among hosts and the fraction of the host population suffering disease mortality as bivariate functions of δ_ν and q_{12} . Both plots follow patterns in the count of stage-1 patches. As we found for structured transmission, disease-mortality frequency is maximal where the frequency of resistance is also maximal (low q_{12} and high δ_ν) because killer patches remove so many susceptibles. The number of stage-2 patches is low where the absolute and relative abundance of resistance is maximal. As we found for structured transmission, vaccinators are not affecting the dynamics significantly.

Our analysis constrains stage-specific virulences, so that $\nu_{\sigma,1} + \nu_{\sigma,2} = 2\nu_0$. Along this constraint, $\partial \mathfrak{M} / \partial \nu_{\sigma,1}$ has the sign of:

$$\phi_\nu = \frac{1 - e^{-\beta_1}}{1 - e^{-\beta_2}} - \frac{q_{12}\xi_1}{1 - \xi_2} \quad (18)$$

Clearly, increasing q_{12} can make pathogen extinction more likely, as in our example. In symmetry with our analysis of ϕ_β , there is always a between-stage transmission ratio (β_1/β_2) large enough to insure that $\phi_\nu > 0$.

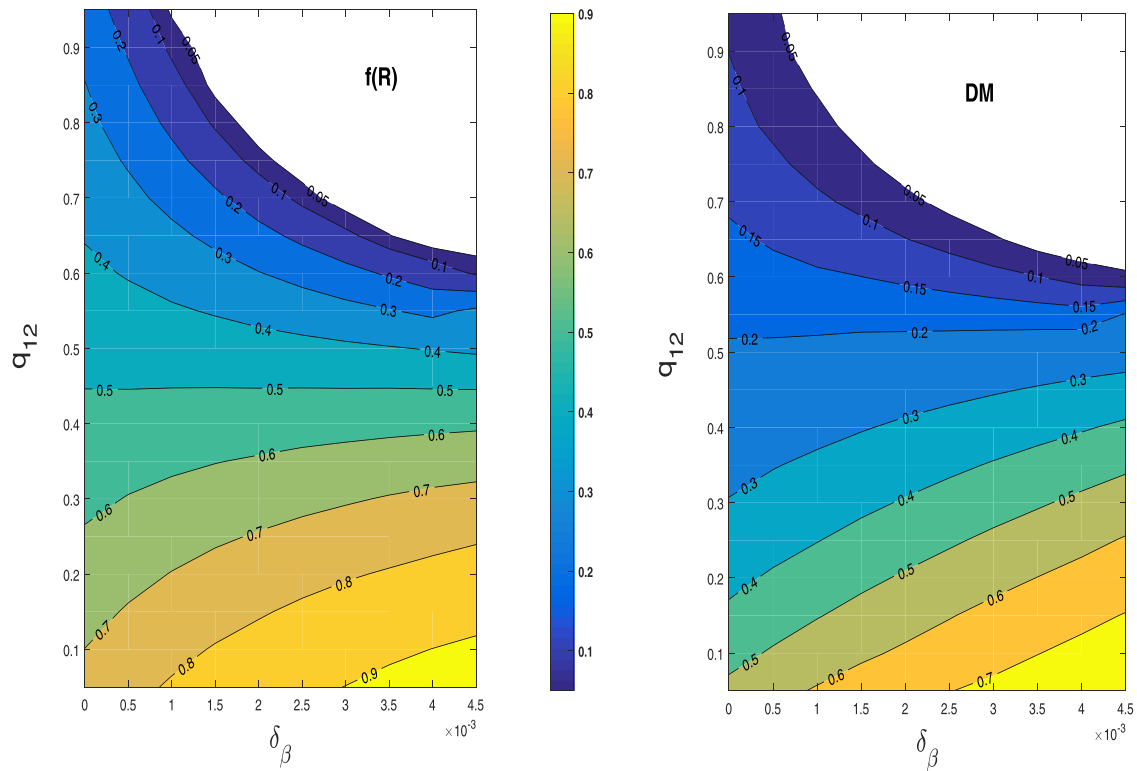


Fig. 4. Resistance frequency and disease mortality frequency under structured transmission. Parameters values from Fig. 3. f(R): fraction of hosts with resistance at start of dry season. DM: fraction of host population suffering disease mortality during annual cycle. Frequencies increase from dark to light colors; pathogen extinct in white area.

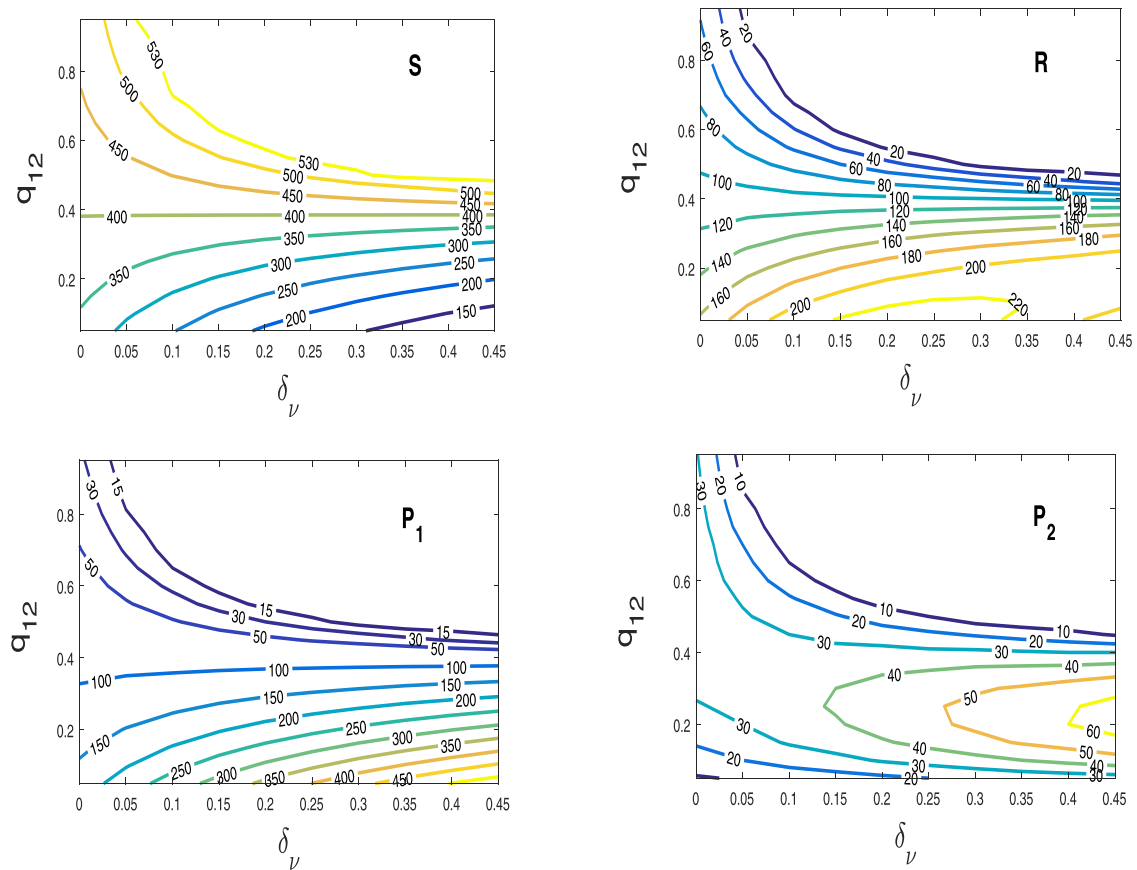


Fig. 5. Structured virulence. Contours: equilibrium susceptible count (upper left), resistant hosts (upper right), first-stage patches (lower left), and second-stage patches (lower right). $v_{\sigma,1} = 0.5 + \delta_\nu$, $v_{\sigma,2} = 0.5 - \delta_\nu$, $v_{\rho,x} = 2v_{\sigma,x}/5$. Each plot: $\lambda = 3$, $\mu = 0.005$, $g = \gamma = 0.8$, $\beta_1 = 0.005$; $\beta_2 = 0.004$. $\xi_1 = \xi_2 = 0.5$, Upper right, each plot: disease-free equilibrium.

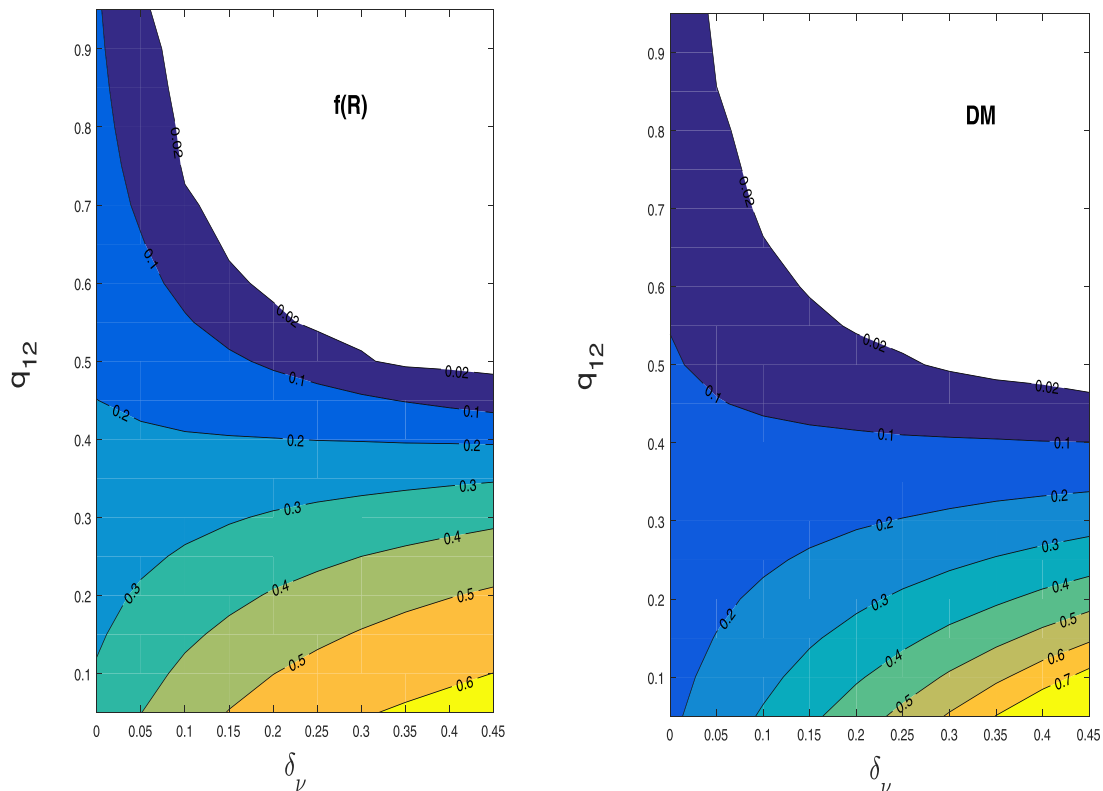


Fig. 6. Resistance frequency and disease mortality frequency under structured virulence. Parameters values from Fig. 5 f(R): fraction of hosts with resistance at start of dry season. DM: fraction of host population suffering disease mortality during annual cycle. Frequencies increase from dark to light colors; pathogen extinct in white area.

7. Virulence-stage transition dependence

Most free-living pathogens do not increase in number outside an infected host. Hence the concentration of pathogen propagules can only decline across seasons. Temperature fluctuations, desiccation, and ultraviolet exposure might accelerate spore-concentration losses observed in nature (Turner et al., 2016) and, in our model's terms, hasten patch transition to the less infectious, less virulent stage. Some pathogen strains might exhibit greater environmental persistence, perhaps by reducing metabolic expenditures after sporulation (Setlow, 2007). However, a spore's physical structures that increase environmental survival may reduce the pathogen's growth rate after ingestion by a host (Leblanc and Lefebvre, 1984), and so reduce the probability that the infection will prove fatal. That is, patches of more virulent pathogen strains may experience the faster decline in spore concentration. Mediated by impacts on within-host growth rate, we can envision positive association of virulence in stage-1 patches and the between-stage transition probability q_{12} . Here, we assume this sort of functional dependence, and ask if it alters the general patterns noted above in population counts and host regulation via disease mortality.

To implement our assumption, we let $q_{12} = v_{\sigma,1}^{\omega}$, where $\omega > 0$. As above, we take $v_{\rho,x} = kv_{\sigma,x}$. Given the functional dependence of q_{12} on virulence in stage-1 patches, we do not require that $(v_{\sigma,1} + v_{\sigma,2})$ remains constant.

Fig. 7 shows exemplary host and patch counts as bivariate functions of $v_{\sigma,1}$ and $v_{\sigma,2}$. At most interior equilibria, increasing $v_{\sigma,1}$ increases susceptible counts and decreases numbers of both resistant hosts and stage-1 patches; the response of stage-2 patches to $v_{\sigma,1}$ is non-monotonic. The counter-intuitive increase in susceptibles and decrease in resistant hosts as killers become more virulent (and $v_{\sigma,2}$ remains constant) reflects the increase in q_{12} with $v_{\sigma,1}$. The increase in between-stage transition outweighs the in-

crease in virulence; stage-1 patches decline at higher $v_{\sigma,1}$, as does the frequency of disease mortality among hosts (see Fig. 8).

Increasing $v_{\sigma,2}$ decreases susceptibles, and increases both resistant hosts and stage-1 patches. Because of the functional dependence between q_{12} and $v_{\sigma,1}$, the combination of high virulence in killer patches and low virulence in vaccinator patches leads to pathogen extinction, and the host population rests at the disease-free equilibrium (Fig. 7).

8. Discussion

Most obligate-killing pathogens release infectious propagules only after the diseased host's death (Ebert and Herre, 1996). Limited dispersal of the free-living stage implies that age or stage structure of the resulting infectious patches should influence pattern in both host exposure to the pathogen and the probability of lethal infection following exposure (Rohani et al., 2009). Given a reasonable, transmission-virulence structure across patches, our model's host population experiences self-regulated natality, followed by exposure to the pathogen, during each annual cycle. A different temporal organization of demographic processes could alter relative strengths of competition and disease in regulating host growth (Abrams, 2009; Cavalieri and Kocak, 1999). Similarly, increased complexity of transmission processes, as observed in avian influenza (Rohani et al., 2009), can alter the host-parasite dynamics profoundly.

The model's point equilibria transition logically from the disease-free state to host-pathogen coexistence. This study's first general objective was demonstrating how between-stage epidemiological variation can impact host and pathogen-patch numbers. We therefore let between-stage difference in transmission, and then the between-stage difference in virulence, increase independently of other parameters. Effects of increasing either between-

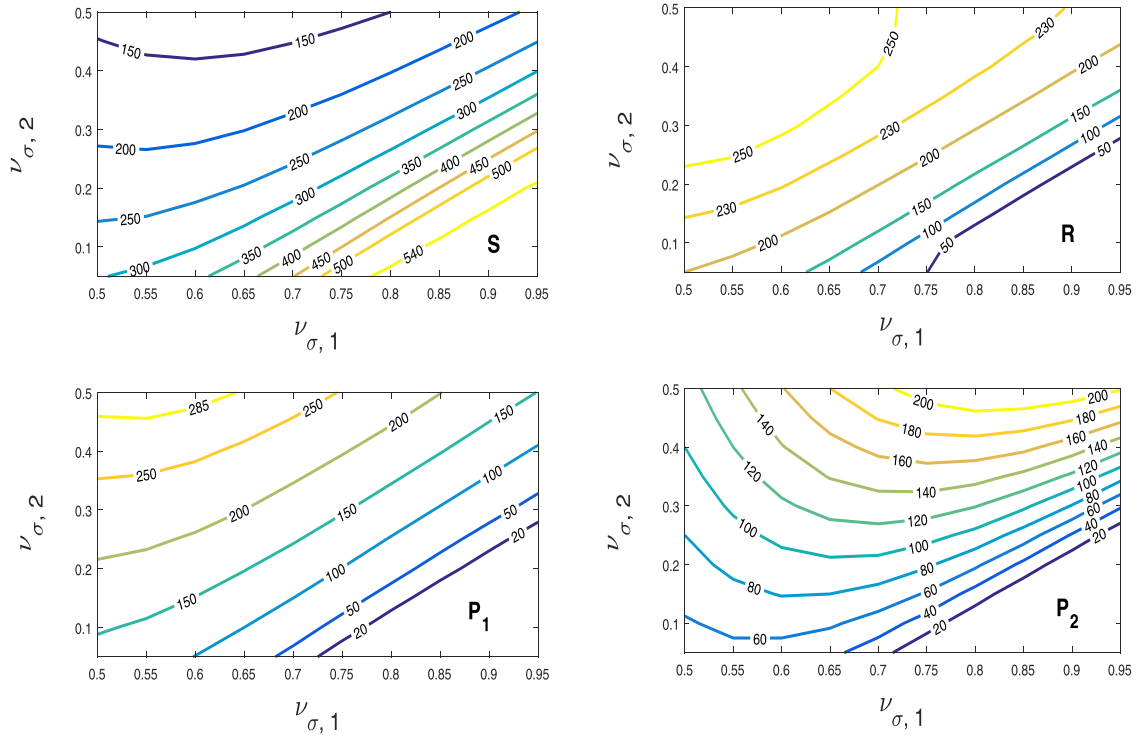


Fig. 7. Virulence, stage-transition correlation. $\beta_1 = 0.006$, $\beta_2 = 0.004$, $k = 0.5$; $\omega = 2$, $\lambda = 3$; $\mu = 0.005$; $g = \gamma = 0.8$, $\xi_1 = \xi_2 = 0.6$. Lower right, each plot: disease-free equilibrium.

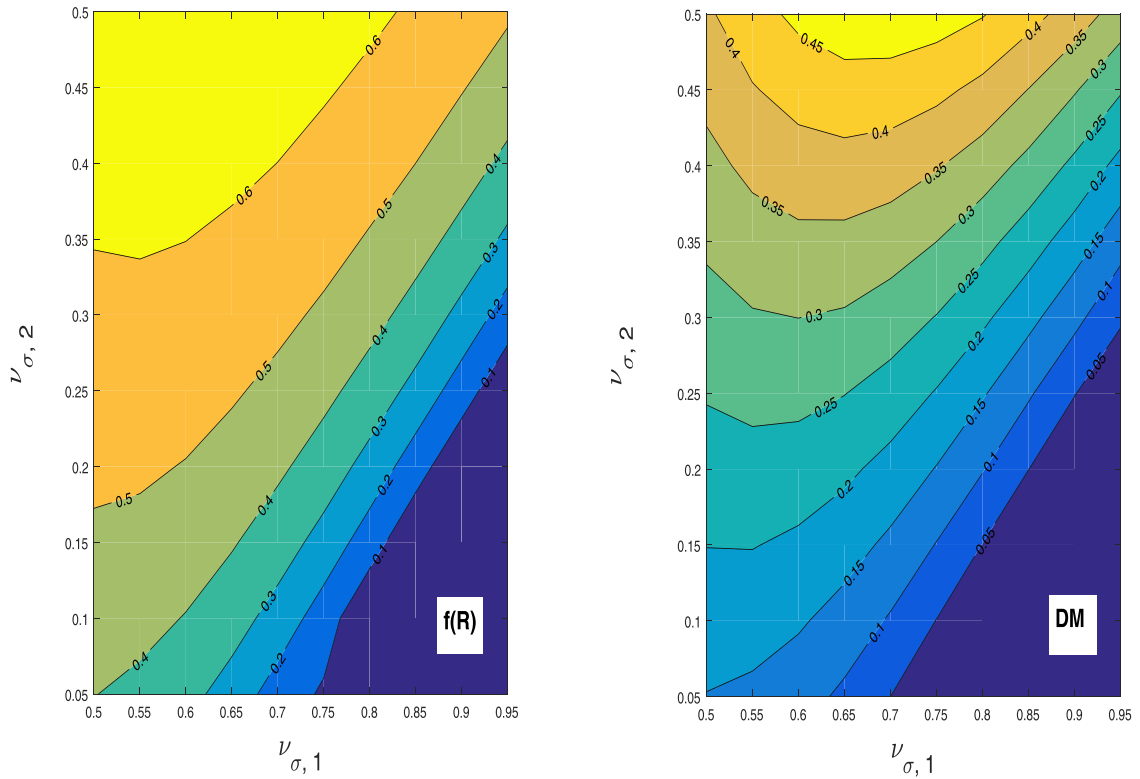


Fig. 8. Resistance frequency and disease mortality frequency when $v_{\sigma, 1}$ and q_{12} functionally dependent. Parameters values from Fig. 7. $f(R)$: fraction of hosts with resistance at start of dry season. DM: fraction of host population suffering disease mortality during annual cycle. Frequencies increase from dark to light colors; pathogen extinct in lower right corner.

stage difference (about a fixed mean) depended on the probability a pathogen patch transitions from the first to second stage (q_{12}), the chance that a killer becomes a vaccinator during the dry season. Though not reported in this paper, qualitatively similar patterns can be produced by varying the ξ_x , stage-specific patch survival through the dry season. Stage-specific survival differences directly influence the $P_{x,t}$, and so indirectly influence the system's response to between-stage differences in transmission or virulence. For completeness, analytical approximation indicates that the reversal of effects of structured transmission at high q_{12} need not occur if killer patches are sufficiently more virulent than stage-2 patches. Similarly, reversal of virulence-difference effects at high q_{12} can be limited if hosts visit stage-2 patches very rarely, since natural vaccination then declines. More interestingly, by assuming functional dependence between virulence in stage-1 patches and q_{12} , we found that the impact of increasingly virulent killers can be pathogen extinction.

Our second focal objective concerned the role of lower-virulence patches in the host-pathogen dynamics. The killer-vaccinator distinction can imply that resistance among hosts should increase, and disease mortality could decline, when the frequency or density of vaccinator patches increases. In our model patches originate as killers, and some persist long enough to become vaccinators; the dynamics does, however, admit equilibria where vaccinators outnumber killers. Under both increasing transmission structure and increasing virulence structure, we found that the frequency of resistance increased with the absolute and relative abundance of killers. Hence resistance was most common when disease mortality was maximal. Many hosts acquire resistance *via* the more attractive, more numerous, and more virulent, stage-1 patches.

The preceding conclusion is premised by our assumptions that $\beta_1 > \beta_2$, and $\xi_1 \geq \xi_2$. Pathogen transmission should be greater at more recent patches, where spore concentrations will be larger. More recent patches should be no more susceptible to loss through local fluctuations in abiotic factors than are older patches (Allstadt et al., 2007). Relaxing these assumptions necessarily permits a wider range of model behavior.

8.1. Directions

Our study focuses on two ecological problems directly suggested by temporal decline in spore-density observed at *B. anthracis* patches (Turner et al., 2016). The initial stage of our patches attracts mobile hosts at a relatively high rate, and kills a relatively large proportion of hosts infected. The life history of an infectious patch, as we model it, contrasts with the life history envisioned in recent models for stage-structured predation (Xiao and Chen, 2004). Adult/experienced (vertebrate) predators ordinarily attack, capture and consume prey more frequently than do juvenile/inexperienced predators. Consequently, the juvenile to adult transition as a predator ages implies an increase in that individual's rate of prey capture (Georgescu et al., 2010). Aging predators take more victims, but aging pathogen patches infect fewer hosts.

Our ecological model might be extended to the adaptive dynamics of pathogen-strain competition. Given a resident strain at endemic equilibrium, one can ask if a rare mutant strain (different phenotype) can invade (van Baalen and Sabelis, 1995). If an environmentally transmitted pathogen does not reproduce in the abiotic environment, successful mutations should arise during the period of within-host growth. If strain competition within the host always leads to exclusion of one strain before the host dies (Caraco et al., 2006), each new patch will contain a single pathogen strain. Consequently, transmission competition will occur only at the among-patch scale. However, if within-host competition allows resident and mutant strains to coexist, or if the host dies before either strain is excluded, new patches will contain multiple strains, differing in phenotypes, complicating both the patch's life history and the transmission/virulence characteristics of infections at the patches (van Baalen and Sabelis, 1995).

Acknowledgment

We thank the reviewers for their insightful comments on the paper; their concerns led to substantial improvements.

Appendix A. Host self-regulation and pathogen extinction

Fig. 9 shows numbers of susceptible and resistant hosts, and numbers of the patch stages, as intra-specific competition grows

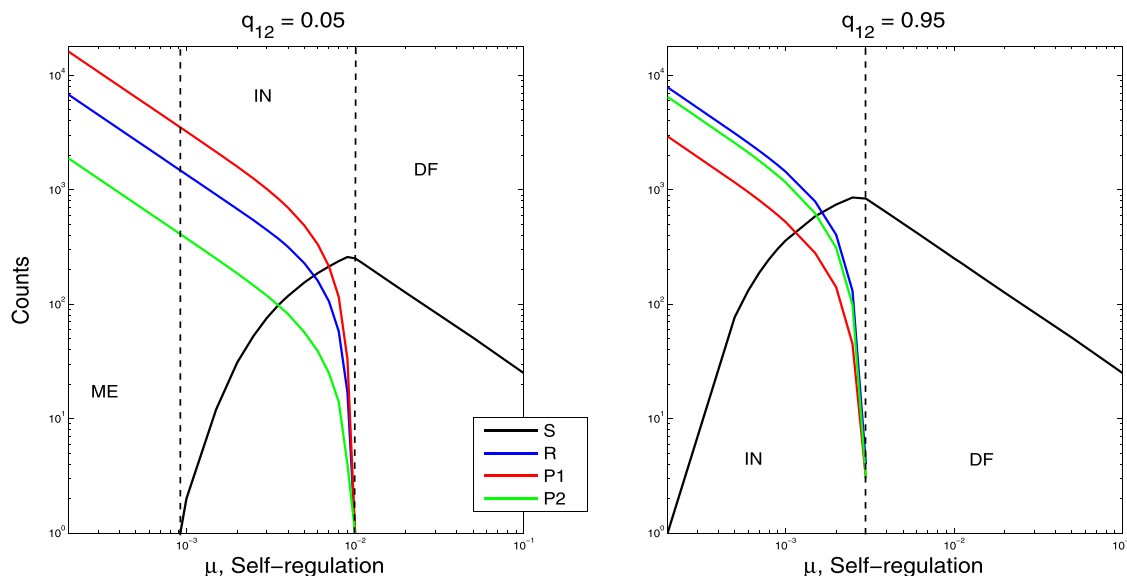


Fig. 9. Increasing host self-regulation. Abscissa: μ (log scaling); self-regulation stronger as μ increases. Ordinate: Host and pathogen-patch numbers (log scaling); see legend. Point equilibria: maximal exposure (ME), interior (IN), and disease-free (DF). Both plots: $\lambda = 2.5$, $g = 0.8$, $\gamma = 0.8$, $\beta_1 = 0.003$, $\beta_2 = \beta_1/2$; $\xi_1 = \xi_2 = 0.7$, $\nu_{\sigma,1} = 0.6$, $\nu_{\sigma,2} = 0.3$, $\nu_{\rho,1} = 0.4$, $\nu_{\rho,2} = 0.1$. Left plot: $q_{12} = 0.05$. Right plot: $q_{12} = 0.95$. Equilibria locally stable (numerical checks).

stronger. In the left plot, transition from the first to second patch-stage is delayed ($q_{12} = 0.05$), and $P_1^* > P_2^*$. In the right plot, the between-stage transition is rapid ($q_{12} = 0.95$), and the pathogen's stage structure is inverted, $P_2^* > P_1^*$.

The two plots in Fig. 9 share qualitative properties. Weak self-regulation, relative to density-dependent disease mortality, allows large numbers of pathogen patches and, correspondingly, the absolute number and relative frequency of resistant hosts are large. Stronger self-regulation (i.e., as competition limits the degree of overcompensation), reduces counts of both patch stages and the number of resistant hosts. Simultaneously, the number of susceptibles grows - but total host number ($S^* + R^*$) declines; hence, the frequency of resistance declines rapidly as the intensity of intraspecific competition, relative to disease regulation, increases. As long as the pathogen remains extant, the total number of hosts falls short of the disease-free equilibrium (the “carrying capacity”) for given μ . Sufficiently strong self-regulation produces pathogen extinction, and resistant hosts consequently disappear. The number of susceptible hosts grows as μ increases until the disease-free state emerges. Thereafter, the host population must decline with stronger self-regulation.

Differences between plots follow from pathogen-patch structure. The transitions from the maximal-exposure to interior equilibrium, and from the interior to disease-free equilibrium, occur at lower levels of self-regulation as the frequency of the less virulent, second-stage patches increases (larger q_{12}). Overall, the model's density-dependent regulation of host numbers responds strongly to pathogen-patch structure.

Appendix B. Infectious patches without structure

The unstructured dynamics assumes identical infectious patches. Then:

$$S_{t+1} = e^{-\beta_0 \pi_0 t} ([S_t + R_t] [g + \lambda e^{-\mu(S_t + R_t)}]) \tag{B.1}$$

$$R_{t+1} = [1 - e^{-\beta_0 \pi_0 t}] \{ [g(S_t + \gamma R_T) + \lambda(S_t + R_t) e^{-\mu(S_t + R_t)}] [1 - \nu_{\sigma,0}] + g(1 - \gamma)R_t [1 - \nu_{\rho,0}] \} \tag{B.2}$$

$$P_{0,t+1} = \xi_0 P_{0,t} + [1 - e^{-\beta_0 \pi_0 t}] \{ [g(S_t + \gamma R_T) + \lambda(S_t + R_t) e^{-\mu(S_t + R_t)}] \nu_{\sigma,0} + g(1 - \gamma)R_t \nu_{\rho,0} \} \tag{B.3}$$

The subscript 0 refers to the unstructured dynamics. $P_{0,t}$ is the number of identical pathogen patches in the dry season. π_0 counts patches during the wet season; $\pi_0 = \xi_0 P_{0,t}$. If we set $\beta_0 = \beta_1 + \beta_2$, we fix transmission events per host, per patch, between the structured and unstructured cases. Virulences $\nu_{\sigma,0}$ and $\nu_{\rho,0}$ can be chosen for the same purpose. We also can equate a patch's mean “lifetime” for the two cases, so that:

$$(1 - \xi_0)^{-1} = \langle \tau_1 \rangle + \frac{\xi_1 q_{12}}{1 - \xi_1 + \xi_1 q_{12}} \langle \tau_2 \rangle$$

$$= \frac{1}{1 - \xi_1 + \xi_1 q_{12}} \left[1 + \frac{\xi_1 q_{12}}{1 - \xi_2} \right] \tag{B.4}$$

Solving for the unstructured model's patch-survival probability satisfying the constraint on the mean yields:

$$\xi_0 = \xi_1 \frac{1 - \xi_2 + \xi_2 q_{12}}{1 - \xi_2 + \xi_1 q_{12}} \tag{B.5}$$

Note that if $\xi_1 = \xi_2 = \xi$, then $\xi_0 = \xi$, as it must.

In the pathogen's absence, equilibrium density of susceptible hosts must remain $S_{DF}^* = [\ln(\lambda) - \ln(1 - g)]/\mu$. The unstructured pathogen must go extinct if:

$$\mathfrak{R}_0^u = S_{DF}^* (1 - e^{-\beta_0}) \nu_{\sigma,0} / (1 - \xi_0) < 1 \tag{B.6}$$

Appendix C. Disease-free dynamics

In the disease-free dynamics, increasing host natality λ generates a cascade of period-doubling bifurcations. Given μ , which scales self-regulation of host reproduction, the locally stable equilibrium node $S^* > 0$ becomes unstable, and a period-2 cycle becomes stable, at the first pitchfork bifurcation; see Fig. 10. We let $\lambda_1(g)$ represent the natality, as a function of dry-season survival g , where the first bifurcation occurs. From the stability criterion for S^* , presented in the text, we have:

$$\lambda_1(g) = (1 - g) \exp\{2/(1 - g)\} \tag{C.1}$$

$\lambda_1(g)$ increases convexly with g , and does not depend on μ .

Fig. 11 shows bifurcation plots for two levels of dry-season survival g . For the lesser level of g , we see the bifurcation cascade. After increasing g , the dynamics bifurcates only once over the same range of λ . Given natality λ , increasing dry-season survival first delays, and then can eliminate, complex dynamics (Kaitala et al., 1999; Ruxton and Rohani, 1998; Trainor and Caraco, 2006).

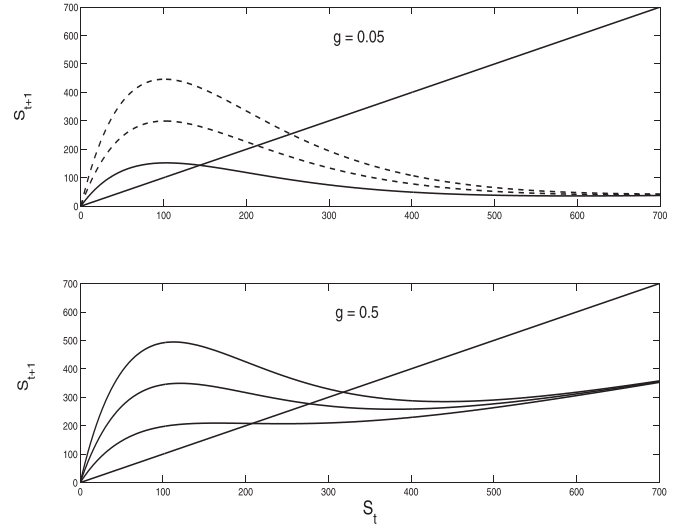


Fig. 10. Disease-free host dynamics. At equilibrium, $S_{t+1} = S_t$. In each plot the positive equilibrium node S^* increases with host natality $\lambda = 4, 8, 12$. Upper plot: Low dry-season survival generates strong overcompensation. Broken 1-D maps (for $\lambda = 8$ and 12) indicate S^* unstable. Lower plot: Increased dry-season survival both increases and stabilizes positive equilibrium nodes for the same natality levels. $\mu = 0.01$ for each map.

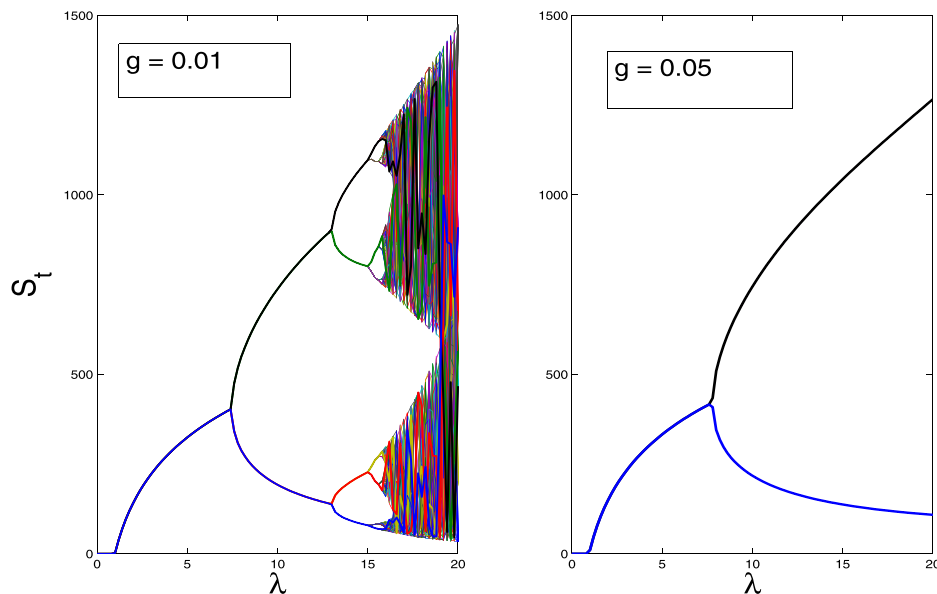


Fig. 11. Dry-season survival and chaos. Bifurcation plots; $\mu = 0.005$ in each. Each plot shows susceptible population sizes for times $t = 251$ through $t = 2000$. Left plot: $g = 0.01$; period-doubling bifurcations, with increasing λ , take the dynamics to chaos. Right plot: $g = 0.05$; increased survival delays onset of complex dynamics.

References

- Abrams, P.A., 2009. When does greater mortality increase population size? The long history and diverse mechanisms underlying the hydra effect. *Ecol. Lett.* 12, 464–474.
- Alizon, S., Michalakis, Y., 2015. Adaptive virulence evolution: the good old fitness-based approach. *Trends in Ecol. Evol.* 30, 248–254.
- Allstadt, A., Caraco, T., Korniss, G., 2007. Ecological invasion, spatial clustering and the critical radius. *Evol. Ecol. Res.* 9, 375–394.
- Avilés, L., 1999. Cooperation and non-linear dynamics: an ecological perspective on the evolution of sociality. *Evol. Ecol. Res.* 1, 459–467.
- van Baalen, M., Sabelis, M.W., 1995. The dynamics of multiple infection and the evolution of virulence. *Am. Nat.* 146, 881–910.
- Bagamian, K.H., Alexander, K.A., Hadfield, T.L., Blackburn, J.K., 2013. Ante- and post-mortem diagnostic techniques for anthrax: rethinking pathogen exposure and the geographic extent of the disease in wildlife. *J. Wild. Dis.* 49, 786–801.
- Breban, R., Drake, J.M., Rohani, P., 2010. A general multi-strain model with environmental transmission: invasion conditions for the disease-free and endemic states. *J. Theor. Biol.* 264, 729–736.
- Caraco, T., Cizauskas, C.A., Wang, I.-N., 2016. Environmentally transmitted parasites: host-jumping in a heterogeneous environment. *J. Theor. Biol.* 397, 33–42.
- Caraco, T., Glavanakov, S., Li, S., Maniatty, W., Szymanski, B.K., 2006. Spatially structured superinfection and the evolution of disease virulence. *Theor. Pop. Biol.* 69, 367–384.
- Caraco, T., Wang, I.-N., 2008. Free-living pathogens: life-history constraints and strain competition. *J. Theor. Biol.* 250, 569–579.
- Caraco, T., Yousefi, A., Wang, I.-N., 2014. Host-jumping, demographic stochasticity and extinction: lytic viruses. *Evol. Ecol. Res.* 16, 551–568.
- Cavaliere, I., Kocak, H., 1999. Comparative dynamics of three models for host-parasitoid interactions in a patchy environment. *Bull. Math. Biol.* 61, 141–155.
- Cizauskas, C.A., Bellan, S.E., Turner, W.C., Vance, R.E., Getz, W.M., 2014. Frequent and seasonally viable sublethal anthrax infections are accompanied by short-lived immunity in an endemic system. *J. Anim. Ecol.* 83, 1078–1090.
- Cressler, C.E., McLeod, D.W., Rozins, C., Hoogen, J.V.d., Day, T., 2015. The adaptive evolution of virulence: a review of theoretical predictions and empirical tests. *Parasitology* 16, 16. doi:10.1017/S003118201500092X.
- Day, T., 2002. Virulence evolution via host exploitation and toxin production in spore-producing pathogens. *Ecol. Lett.* 5, 471–476.
- Duryea, M., Caraco, T., Gardner, G., Maniatty, W., Szymanski, B.K., 1999. Population dispersion and equilibrium infection frequency in a spatial epidemic. *Physica D* 132, 569–579.
- Dwyer, G., 1992. On the spatial spread of insect viruses: theory and experiment. *Ecology* 73, 479–494.
- Dwyer, G., 1994. Density dependence and spatial structure in the dynamics of insect pathogens. *Am. Nat.* 143, 533–562.
- Ebert, D., Herre, E.A., 1996. The evolution of parasitic diseases. *Parasit.* 12, 96–100. Today
- Friedman, A., Yakubu, A.-A., 2013. Anthrax epizootic and migration: persistence or extinction. *Math. Biosci.* 241, 137–144.
- Gandon, S., 1998. The curse of the pharaoh hypothesis. *Proc. R. Soc. Lond. B* 265, 1545–1552.
- Gasaway, W.C., Gasaway, K.T., Berry, H.H., 1996. Persistent low densities of plains ungulates in etosha national park, namibia: testing the food-regulation hypothesis. *Can. J. Zool.* 74, 1556–1572.
- Georgescu, P., Hsieh, Y.-H., Zhang, H., 2010. A lyapunov functional for a stage-structured predator-prey model with nonlinear predation rate. *Nonlin. Analysis: Real World Appl.* 11, 3653–3665.
- Godfray, H.C.J., O'Reilly, D.R., Briggs, C.J., 1997. A model of nucleopolyhedrovirus (NPV) population genetics applied to co-occlusion and the spread of the few polyhedra (FP) phenotype. *Proc. R. Soc. Lond. B* 264, 315–322.
- Havarua, Z., Turner, W.C., Mfunne, J.K.E., 2014. Seasonal variation in foraging behavior of plains zebras (*Equus quagga*) may alter contact with the anthrax bacterium (*Bacillus anthracis*). *Canadian J. Zool.* 92, 331–337.
- Kaitala, V., Ylikarjula, J., Heino, M., 1999. Dynamic complexities in host-parasitoid interaction. *J. Theor. Biol.* 197, 331–341.
- Kaplan, D., Glass, L., 1995. Understanding Nonlinear Dynamics. Springer-Verlag, New York USA.
- Leblanc, R., Lefebvre, G.M., 1984. A stochastic model of bacterial spore germination. *bull. Math. Biol.* 46, 447–460.
- May, R.M., Hassell, M.P., Anderson, R.M., Tonkyn, D.W., 1981. Density dependence in host-parasitoid models. *J. Anim. Ecol.* 50, 855–865.
- McCauley, E., Wilson, W.G., de Roos, A.M., 1993. Dynamics of age-structured and spatially structured predator-prey interactions: individual-based models and population-level formulations. *Am. Nat.* 142, 412–442.
- Moore, S.M., Shannon, K.L., Zelaya, C.E., Azman, A.S., Lessler, J., 2014. Epidemic risk from cholera introductions into mexico. *PLoS Currents: Outbreaks* 17. doi:10.1371/currents.outbreaks.c04478c7fbd9854ef6ba923cc81eb799.
- Pujol, J.M., Eisenberg, J.E., Haas, C.N., Koopman, J.S., 2009. The effect of ongoing exposure dynamics in dose response relationships. *PLoS Comp. Biol.* 5, 12. E1000399.
- Reeson, A.F., Wilson, K., Cory, J.S., Hankard, P., Weeks, J.M., Goulson, D., Hails, R.S., 2000. Effects of phenotypic plasticity on pathogen transmission in the field in a lepidoptera-NPV system. *Oecologia* 124, 373–380.
- Roche, B., Drake, J.M., Rohani, P., 2011. The curse of the pharaoh revisited: evolutionary bi-stability in environmentally transmitted pathogens. *Ecol. Lett.* 7. doi:10.1111/j.1461-0248.2011.01619.x.
- Rohani, P., Breban, R., Stallknecht, D.E., Drake, J.M., 2009. Environmental transmission of low pathogenicity avian influenza viruses and its implications for pathogen invasion. *PNAS* 106, 10365–10369.
- Ruxton, G.D., Rohani, P., 1998. Population floors and the persistence of chaos in ecological models. *Theor. Pop. Biol.* 53, 175–183.
- Setlow, P., 2007. I will survive: DNA protection in bacterial spores. *Trends Microbiol.* 15, 172–180.
- Sinclair, A.R.E., Maduma, S.A.R., Arcese, P., 2000. What determines phenology and synchrony of ungulate breeding in serengeti? *Ecology* 81, 2100–2111.
- Trainor, K.T., Caraco, T., 2006. Group size, energy budgets, and population dynamic complexity. *Evol. Ecol. Res.* 8, 1173–1192.
- Turnbull, P.C.B., 2008. Anthrax in humans and animals, fourth ed. World Health Organization, Geneva, Switzerland.
- Turner, J., Bowers, R.G., Begon, M., Robinson, S.E., French, N.P., 2006. A semi-stochastic model of the transmission of escherichia coli o157 in a typical UK dairy herd: dynamics, sensitivity analysis and intervention/prevention strategies. *J. Theor. Biol.* 241, 806–822.

- Turner, W.C., Imologhome, P., Havarua, Z., Kaaya, G.P., Mfunu, J.K.E., Mpofo, I.D.T., Getz, W.M., 2013. Soil ingestion, nutrition, and the seasonality of anthrax in herbivores of etosha national park. *Ecosphere* 4 (13), 19.
- Turner, W.C., Kausrud, K.L., Beyer, W., et al., 2016. Lethal exposure: an integrated approach to pathogen transmission via environmental reservoirs. *Sci. Reports* 6, 13. 27311
- Turner, W.C., Kausrud, K.L., Krishnappa, Y.S., Cromsigt, J.P.G.M., Ganz, H.H., Mapaire, I., Cloete, C.C., Havarua, Z., Küsters, M., Getz, W.M., Stenseth, N.C., 2014. Fatal attraction: vegetation responses to nutrient inputs attract herbivores to infectious anthrax carcass sites. *Proc. Roy. Soc. B* 281.
- Walther, B., Ewald, P.W., 2004. Pathogen survival in the external environment and the evolution of virulence. *Biol. Rev. Camb. Philos. Soc.* 79, 849–869.
- Xiao, Y.N., Chen, L., 2004. Global stability of a predator-prey system with stage structure for predator. *Acta. Math. Sin.* 20, 63–70.